Use of the Novel Fluorescent Amino Acid *p*-Cyanophenylalanine Offers a Direct Probe of Hydrophobic Core Formation during the Folding of the N-Terminal Domain of the Ribosomal Protein L9 and Provides Evidence for Two-State Folding†

Konstantinos N. Aprilakis,‡,§ Humeyra Taskent,‡,§ and Daniel P. Raleigh*,‡,||

Department of Chemistry, State University of New York at Stony Brook, Stony Brook, New York 11794-3400, Institute for Chemical Biology and Drug Discovery, State University of New York at Stony Brook, Stony Brook, New York 11794-3400, and Graduate Program in Biochemistry and Structural Biology, State University of New York at Stony Brook, Stony Brook, New York 11794-3400

Received May 31, 2007; Revised Manuscript Received August 13, 2007

ABSTRACT: Fluorescence-detected stopped flow measurements are the method of choice for studies of protein folding kinetics. However, the methodology suffers from the limitation that the protein of interest either must contain an intrinsic fluorophore or can tolerate its introduction by mutagenesis. Recently, the cyano (nitrile) analogue of phenylalanine has been proposed for use as a fluorescence analogue. Here we take advantage of this new methodology to monitor the formation of the hydrophobic core during the folding of the N-terminal domain of L9 (NTL9). Phenylalanine 5, which is completely buried in the folded state of NTL9, was replaced with *p*-cyanophenylalanine (*p*-cyano-Phe). This derivative reports on the formation of the hydrophobic core. The variant adopts the same fold as wild-type NTL9 and is slightly more stable. Refolding and unfolding were monitored using both guanidine HCl and urea jump experiments. In both cases, plots of the natural log of the observed relaxation rate versus denaturant concentration, so-called chevron plots, exhibited the characteristic V shape expected for two-state folding, and no hint of deviation from linearity was observed at low denaturant concentrations. The stability calculated from the measured folding and unfolding rates is in very good agreement with the value obtained from equilibrium measurements as is the *m* value. The relative compactness of the transition state for folding as defined by the Tanford β parameter is identical to that of the wild type. The results illustrate the applicability of *p*-cyano-Phe analogues in protein folding studies and provide further evidence of two-state folding of NTL9.

Protein folding is an extremely active area of research, motivated both by the desire to decipher the code which links primary sequence and function and by the importance of protein misfolding in biotechnology and human health (*1*−*7*). Probably the most widely applied experimental method for the direct study of folding and unfolding kinetics is fluorescence-detected stopped flow measurement (*3*). Such studies rely on the presence of a tryptophan or tyrosine residue which experiences a significant change in fluorescence upon unfolding. The method, although very powerful, does suffer from the requirement for an intrinsic fluorophore or depends upon the ability of the protein to tolerate the introduction of tryptophan or tyrosine at a suitable position. Recently, the cyano (nitrile) analogue of phenylalanine (*p*-cyano-Phe)[1] has been proposed for use as a fluorescence probe of folding and of binding (*8*). The fluorescent quantum yield of the *p*-cyano-Phe side chain is very sensitive to interaction with solvent and is increased significantly in H_2O relative to its value in organic solvents. Thus, *p*-cyano-Phe fluorescence is an attractive probe of hydrophobic core formation. The side chain of *p*-cyano-Phe has two absorption maxima in the UV at approximately 233 and 280 nm. This allows *p*-cyano-Phe to be selectively excited at 240 nm even in the presence of Trp and Tyr (*9*). The fluorescence emission of *p*-cyano-Phe overlaps with the Trp absorption band, and *p*-cyano-Phe and Trp have been shown to form a useful FRET pair. *p*-Cyano-Phe also has an attractive feature in that the cyano group, while a H-bond acceptor, can be readily tolerated in the hydrophobic core since it has a polarity between that of a methylene group and that of an amide (*8*, *10*, *11*). It is also considerably smaller than Trp and is less polar than Tyr, making it a more conservative replacement for Phe.

In this work, we use *p*-cyano-Phe fluorescence as a probe of hydrophobic core formation during the folding of an $\alpha-\beta$ protein, the N-terminal domain of ribosomal protein L9

† Supported by NIH Grant GM70941 to D.P.R.

* To whom correspondence should be addressed. Phone: (631) 632-9547. Fax: (631) 632-7960. E-mail: draleigh@notes.cc.sunysb.edu.

‡ Department of Chemistry.

§ These authors contributed equally to this work.

|| Institute for Chemical Biology and Drug Discovery and Graduate Program in Biochemistry and Structural Biology.

[1] Abbreviations: β_T, Tanford β parameter defined by $m_f/(m_f - m_u)$; CD, circular dichroism; $F5F_{C\equiv N}$ NTL9, NTL9 with a *p*-cyanophenylalanine at position 5; k_f, folding rate; k_u, unfolding rate; m_{eqlib}, equilibrium *m* value; m_f, kinetic *m* value for folding; m_u, kinetic *m* value for unfolding; NTL9, N-terminal domain of ribosomal protein L9 comprised of residues 1−56 of intact L9; *p*-cyano-Phe, *p*-cyanophenylalanine.

10.1021/bi7010674 CCC: $37.00
Published on Web 10/09/2007

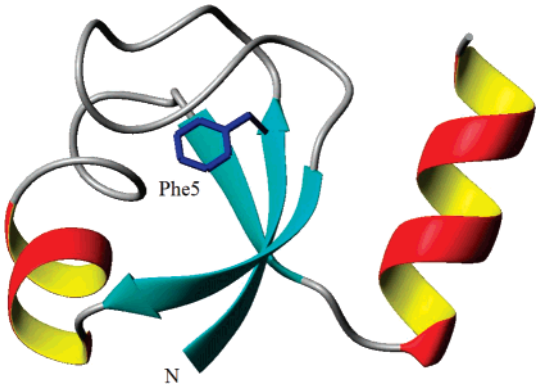

FIGURE 1: Ribbon diagram of NTL9 showing the location of the *p*-cyano-Phe substitution at Phe-5. Phe-5 is completely buried in the native state. The diagram was generated using Protein Data Bank entry 2HBA and MolMol 2K.2.

(NTL9). NTL9 is a relatively small, 56-residue, domain and is the simplest example of a common class of structure, the split $\beta-\alpha-\beta$ motif (*12*−*14*). The domain has been widely used for studies of protein folding and stability (*14*−*18*). Kinetic investigations have relied on the single Tyr found at position 25 since the protein does not contain any Trp residues. Tyr-25 is located on the surface of the protein on the solvent-exposed face of an α-helix. In the native state of NTL9, the Tyr side chain adopts a conformation in which the ring packs against the helix, leaving one face exposed to solvent while shielding the other. This is enough to lead to a change in fluorescence quantum yield between the folded and unfolded states, but the change in fluorescence does not directly report on hydrophobic core formation (*15*). Such a probe would clearly be desirable.

The structure of NTL9 is shown in ribbon format in Figure 1. The topology of the domain is $\beta_1-\beta_2-\alpha_1-\beta_3-\alpha_2$, where the three β-strands form an antiparallel β-sheet and the second helix extends beyond the globular domain to form the connector to the C-terminal domain. Tyr-25 is located on the first helix. The domain is highly soluble, folds and unfolds reversibly over a wide range of conditions, and does not require metal ion or cofactor binding to fold (*14*, *19*). Thus, it is an attractive model system for biophysical investigations. Phenylalanine 5, located on the first β-strand, forms part of the hydrophobic core of the protein and was our target for replacement with *p*-cyano-Phe. The analogue, denoted $F5F_{C\equiv N}$ NTL9, allows hydrophobic core formation during folding to be directly probed.

MATERIALS AND METHODS

Protein Synthesis and Purification. NTL9 incorporating *p*-cyano-Phe was synthesized using Fmoc chemistry on an Applied Biosystems 433A peptide synthesizer. Standard Fmoc protocols were used as described previously (*17*). The *p*-cyano-Phe Fmoc derivative was purchased from EMD Chemicals. The protein was purified using reverse phase HPLC on a Vydac C4 column as described previously (*17*).

Equilibrium Denaturations. CD wavelength scans and CD-monitored denaturation experiments were performed as previously described for NTL9 (*17*). Samples were in 20 mM sodium acetate and 100 mM NaCl. Measurements were conducted at pH 5.4 and 25 °C. *p*-Cyano-Phe fluorescence-monitored denaturation experiments were conducted in 20 mM sodium acetate and 100 mM NaCl (pH 5.4) at 25 °C. *p*-Cyano-Phe fluorescence was excited at 240 nm, and emission was monitored at 297 nm. The concentrations of urea solutions were determined by measuring the refractive index. Denaturation curves were fit to the equation:

$$f = \frac{a_n + b_n[\text{denaturant}] + (a_d + b_d[\text{denaturant}])e^{-[\Delta G^\circ_U([\text{denaturant}]/RT)]}}{1 + e^{-[\Delta G^\circ_U([\text{denaturant}]/RT)]}} \quad (1)$$

Where

$$\Delta G^\circ_U([\text{denaturant}]) = \Delta G^\circ_U(H_2O) - m[\text{denaturant}] \quad (2)$$

and f is the measured signal, (ellipticity in CD and fluorescence signal in fluorescence-monitored denaturation experiments), ΔG°_U is the change in free energy for the unfolding reaction, T is the temperature, and R is the gas constant. a_n is the intercept and b_n the slope of the curve extrapolated in the pretransition region. Similarly, a_d is the intercept and b_d the slope of the curve in the post-transition region.

Stopped Flow Fluorescence Measurements. Stopped flow studies were performed as previously described for NTL9, the exception being that the excitation wavelength was 240 nm (*17*). A 305 nm cutoff filter was used to collect the fluorescence. Samples were in 20 mM sodium acetate and 100 mM NaCl. Measurements were conducted at pH 5.4 and 25 °C. Stopped flow experiments used an 11-fold dilution. The protein concentration before the jump was ∼400 μM. After four to five fluorescence traces were averaged at each denaturant concentration, the average trace was fit to a single-exponential function to obtain the observed rate constant (k_{obs}) at that denaturant concentration. The plot of the natural logarithm of k_{obs} versus denaturant concentration was fit to the following equation:

$$\ln(k_{obs}) = \ln[k_f^{H_2O} \exp(-m_f[\text{denaturant}]/RT) + k_u^{H_2O} \exp(m_u[\text{denaturant}]/RT)] \quad (3)$$

where $k_f^{H_2O}$ and $k_u^{H_2O}$ are the folding and unfolding rates, respectively, in the absence of denaturant.

RESULTS AND DISCUSSION

A *p*-cyano-Phe for Phe replacement is tolerated well at position 5 of NTL9. CD studies (data not shown) demonstrate that the global fold is not perturbed. The location of Phe-5 is shown on the ribbon diagram of Figure 1. Both urea- and guanidine HCl-induced denaturation experiments were used to measure the stability of the domain (Figure 2). The use of denaturant-induced unfolding to measure ΔG° depends upon the validity of the linear extrapolation method (*20*, *21*). The linear extrapolation method has been shown to be valid for NTL9 and for a large number of NTL9 mutants (*17*, *22*). The stability estimated by CD-monitored urea denaturation is 4.67 kcal/mol, while it is 4.71 kcal/mol if guanidine HCl is used. The values are close to those previously determined for the wild type (4.36 kcal/mol) but are slightly larger, although the difference for the urea denaturation experiments is statistically insignificant. In any case, the stability difference is small, showing again that the substitution is tolerated

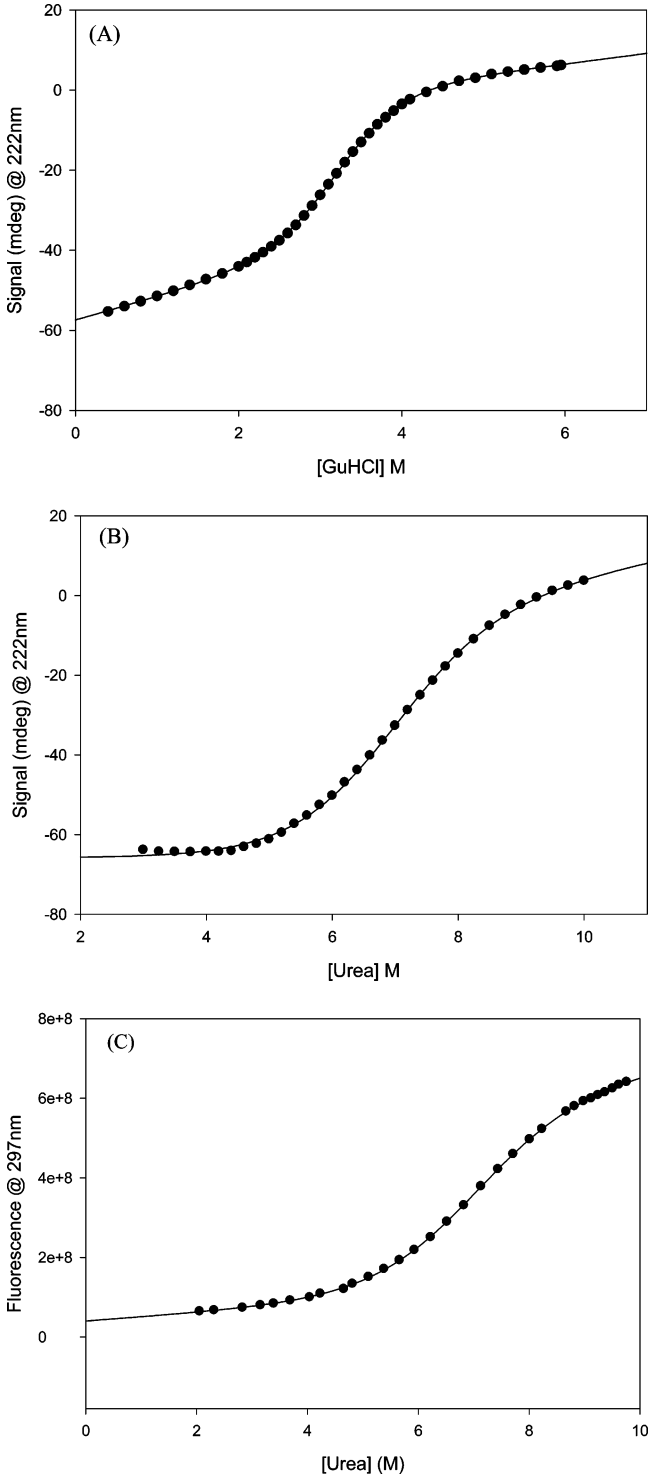

FIGURE 2: Equilibrium unfolding studies of the *p*-cyano-Phe analogue of NTL9. (A) Guanidine HCl-induced unfolding. (B) Urea-induced unfolding. The CD signal at 222 nm was monitored. (C) Urea-induced unfolding monitored by *p*-cyano-Phe fluorescence at 297 nm. Experiments were conducted at pH 5.4 and 25 °C in 20 mM sodium acetate and 100 mM NaCl.

well. We also conducted fluorescence-detected urea unfolding studies. The blue-shifted absorbance of *p*-cyano-Phe allows its fluorescence to be selectively excited at 240 nm and detected in the presence of the single tyrosine. We used urea as the denaturant since chloride is a quencher of *p*-cyano-Phe fluorescence, and this complicates guanidine HCl-induced equilibrium unfolding studies. The stability estimated from the *p*-cyano-Phe fluorescence-monitored studies (4.34 ± 0.36 kcal/mol) is in excellent agreement with the value determined by the CD-monitored unfolding (4.67 ± 0.10 kcal/mol). The *m* values for urea- and guanidine-induced unfolding report on the change in solvent accessible surface area between the native and unfolded states (*23*). The measured values are essentially identical to those previously measured for the wild type, and the values determined by fluorescence and CD are identical within experimental uncertainty. The thermodynamic parameters are summarized in Table 1. The fact that NTL9 tolerates the replacement of a buried phenylalanine without loss of stability or perturbation of the structure illustrates the conservative nature of the *p*-cyano-Phe substitution.

The folding and unfolding kinetics were measured following *p*-cyano-Phe fluorescence using stopped flow methods. A plot of the natural log of the observed first-order rate constant versus denaturant concentration, a chevron plot, is shown in Figure 3. The first panel displays the results of the guanidine jump experiments (Figure 3A), while the second shows the results of the urea jump experiments (Figure 3B). The urea-induced unfolding transitions of both the wild type and $F5F_{C\equiv N}$ NTL9 are rather broad as expected for a protein the size of NTL9. Thus, the guanidine HCl jump studies were conducted to produce the complete chevron plot. The plot displays the classic V-shaped profile expected for cooperative two-state folding. In particular, there is no hint of "rollover", i.e., a deviation from linearity, at low denaturant concentrations. The folding rate obtained from analysis of the data is slightly faster than that of the wild type under the same conditions, while the unfolding rate is slightly slower. However, given the lengthy extrapolation required to estimate the unfolding rate, especially for the urea data, the differences in k_u are unlikely to be significant. The unfolding branch of the urea jump experiment is poorly constructed since it is necessarily defined by a limited number of points; thus, we feel that the estimated k_u is not reliable even though the standard error to the fit is modest. The slightly faster folding is consistent with previous studies that have shown that increasing the size and hydrophobicity of core residues increases the folding rate of NTL9 through stabilization of the transition state via strengthened hydrophobic interactions (*17*). The stability calculated from the measured folding and unfolding rates is in good agreement with the value determined from equilibrium measurements. The chevron plot also yields the dependence of the log of the folding and unfolding rates upon denaturant concentration. These parameters, traditionally denoted as m_f and m_u, respectively, are believed to report on the relative change in accessible surface area between the unfolded state and the transition state (m_f) and between the folded state and the transition state (m_u) (*24*). The values are very similar to those obtained for wild-type NTL9 (*16*, *25*). m_f and m_u can be combined to yield the equilibrium *m* value for unfolding. The value calculated from the kinetic parameters is in excellent agreement with the equilibrium values, consistent with two-state folding. m_f and m_u can also be used to calculate the dimensionless order parameter β_T, also sometimes denoted $\theta_m = [m_f/(m_f - m_u)]$. β_T reports on the relative exposure of the transition state (*24*). Values of ~1 reflect a native-like transition state, while values of ~0 indicate a denatured-like transition state. Most single-domain globular proteins have values between 0.5 and 0.8. For wild-type NTL9, the

Table 1: Comparison of the Measures of Thermodynamic and Kinetic Parameters for WT and $F5F_{C\equiv N}$ NTL9 As Determined by Urea and GuHCl Denaturation[a]

	protein	ΔG_{eqlib} (kcal/mol)	m_{eqlib} (kcal mol^{-1} M^{-1})	k_f (s^{-1})	k_u (s^{-1})	m_f (kcal mol^{-1} M^{-1})	m_u (kcal mol^{-1} M^{-1})	β_T
urea	WT	4.3 ± 0.4[b]	0.7 ± 0.1[b]	900 ± 100[b]	0.9 ± 0.4[b]	0.5 ± 0.1[b]	0.2 ± 0.1[b]	0.7 ± 0.1
	$F5F_{C\equiv N}$	4.7 ± 0.4[c]	0.7 ± 0.1[c]	–	–	–	–	–
	$F5F_{C\equiv N}$	4.3 ± 0.1[d]	0.6 ± 0.1[d]	1000 ± 20	0.3 ± 0.1[e]	0.4 ± 0.1	0.2 ± 0.1[f]	0.7 ± 0.1
GuHCl	WT	4.2 ± 0.1[g]	1.4 ± 0.1[g]	800 ± 40[g]	0.9 ± 0.1[g]	0.9 ± 0.1[g]	0.6 ± 0.1[g]	0.6 ± 0.1
	$F5F_{C\equiv N}$	4.7 ± 0.1	1.45 ± 0.1	1000 ± 30	0.7 ± 0.1	0.9 ± 0.1	0.5 ± 0.1	0.6 ± 0.1

[a] All experiments were conducted in 20 mM NaAc and 100 mM NaCl at 25 °C and pH 5.4. The numbers after the ± symbol are the standard errors to the fit reported to the appropriate number of significant figures. The kinetic data are averages of three to five repeats. The estimated standard deviation for the wild-type equilibrium data is ±0.4 and is based on three repeated measurements. [b] Values taken from ref *16*. [c] Determined by CD-monitored equilibrium unfolding. [d] Determined by *p*-cyano-Phe fluorescence-monitored equilibrium unfolding. [e] The value of k_u for the urea jump experiments with $F5F_{C\equiv N}$ is believed to be unreliable for the reasons described in the text. [f] Calculated using m_{eqlib} and m_f. [g] Values taken from ref *25*.

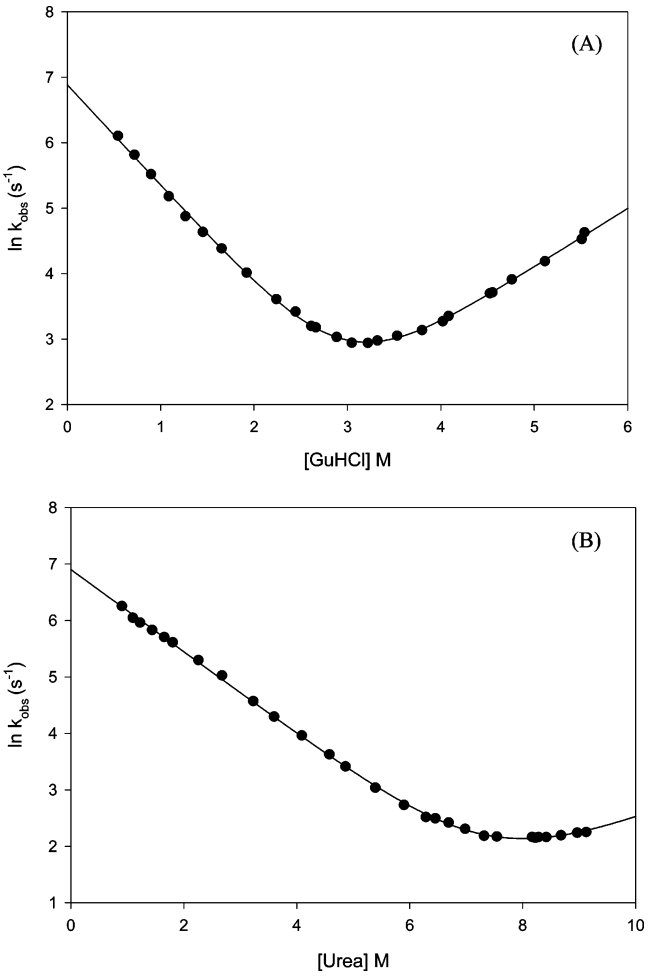

FIGURE 3: Fluorescence-detected stopped flow folding studies of the *p*-cyano-Phe analogue of NTL9. (A) Guanidine HCl jump studies. (B) Urea jump studies. Experiments were conducted at pH 5.4 and 25 °C in 20 mM sodium acetate and 100 mM NaCl.

value of β_T is 0.60−0.65. The *p*-cyano-Phe analogue has a value of 0.63, indicating that, by this measure, the relative position of the transition state has not shifted. The kinetic parameters are included in Table 1.

Chevron plots are based upon the analysis of rates. However, the amplitudes of the stopped flow traces also contain important information. The initial amplitudes, calculated by extrapolating the traces backward to time zero, can be used in a so-called "burst phase" analysis. For two-state folders, the initial amplitudes of refolding studies should fall on the extrapolated baseline for the final intensity at high

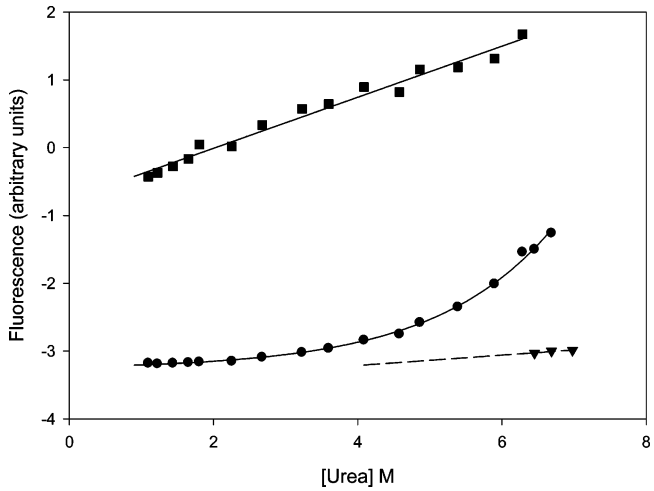

FIGURE 4: Initial (■ and ▼) and final amplitudes (●) from the urea jump stopped flow experiments plotted vs [urea]: (■) refolding studies and (▼) unfolding studies. Experimental conditions were as described in the legend of Figure 3. The initial refolding amplitudes show no deviation from linearity, consistent with the lack of a burst phase intermediate. The solid line is drawn through the initial amplitudes and has no theoretical significance. The dashed line represents extrapolation of the folded baseline.

denaturant concentrations. Stated differently, the initial amplitude in a refolding experiment reports on the fluorescence of an unfolded protein under native conditions. If the fluorescence of the unfolded state is a linear function of denaturant concentration, then one can extrapolate backward to low denaturant concentrations to calculate the expected amplitude for two-state folding. Unfortunately, it is very difficult to conduct a burst phase analysis of the *p*-cyano-Phe derivative. Guanidine HCl quenches the fluorescence of *p*-cyano-Phe; thus, the initial amplitudes are affected by factors other than folding, and the magnitude of this effect varies as a function of guanidine HCl concentration (note that this does not affect the measured rate constants). This is not a problem with urea-induced unfolding. However, the stability and size of NTL9 conspire to prevent the generation of a complete chevron plot. The incomplete unfolding branch prevents a reliable burst phase analysis. Nonetheless, the available data are consistent with the lack of a burst phase. The initial and final amplitudes of the urea jump stopped flow studies are shown in Figure 4. It is not possible to accurately define the unfolded baseline for the reasons outlined above, but the initial amplitudes are a linear function of denaturant concentration. A plot of the initial amplitudes shows no hint of sigmoidal curvature as would be expected

for a burst phase intermediate. We also note that the value of the folding rate determined from the urea chevron plot is in good agreement with the value obtained from the guanidine HCl jump studies. The kinetic data are summarized in Table 1.

CONCLUSIONS

This study demonstrates the utility of *p*-cyano-Phe as a fluorescence probe for protein folding studies. The relatively conservative nature of the cyano substitution should allow the replacement of Phe or Tyr residues. In this study, introduction of the noncoded amino acid at a completely buried position did not alter the structure or stability of the protein.

The probe is particularly useful for studies of hydrophobic core formation given the large fluorescence change observed between an aqueous and hydrophobic environment. The data presented here for NTL9 highlight the conservative nature of a *p*-cyano-Phe for Phe substitution. The use of noncoded amino acids in protein folding studies has been limited to date (*17*, *25*−*28*). We expect this to change rapidly given recent technical advances. Advances in peptide synthesis have made the assembly of small single-domain proteins relatively straightforward (*29*). Larger proteins can be produced using native ligation and expressed protein ligation methodologies (*30*, *31*). In addition, Schultz and co-workers have developed *Escherichia coli* strains for the recombinant production of 4-cyano-Phe-containing proteins (*32*). Thus, incorporation of this useful analogue is relatively straightforward and should become even easier as technology continues to mature.

In the case presented here, use of *p*-cyano-Phe has provided important new information about the folding of NTL9. All previous studies relied upon the fluorescence of the single tyrosine at position 25. This residue is not part of the hydrophobic core and is partially exposed to solvent in the native state. Thus, it does not directly report on the development of the hydrophobic core. In contrast, the kinetic refolding and unfolding experiments conducted with $F5F_{C\equiv N}$ NTL9 report directly on hydrophobic core formation. The data presented here are consistent with cooperative two-state folding of the split $\beta-\alpha-\beta$ motif of NTL9.

ACKNOWLEDGMENT

We thank Ms. BenBen Song for help with peptide synthesis and Professor Feng Gai, Professor Isaac Carrico, and Dr. Jae-Hyun Cho for helpful discussion and for their interest in this work. We also thank Professor Gai for communicating results prior to publication.

REFERENCES

1. Levinthal, C. (1968) Are there pathways for protein folding? *J. Chim. Phys. Phys.-Chim. Biol. 65*, 44−45.
2. Anfinsen, C. B. (1973) Principles that govern folding of protein chains, *Science 181*, 223−230.
3. Fersht, A. R. (2000) *Structure and Mechanism in Protein Science: A Guide to Enzyme Catalysis and Protein Folding*, W. H. Freeman & Co., New York.
4. Onuchic, J. N., Nymeyer, H., Garcia, A. E., Chahine, J., and Socci, N. D. (2000) The energy landscape theory of protein folding: Insights into folding mechanisms and scenarios, *Adv. Protein Chem. 53*, 87−152.
5. Dobson, C. M. (2003) Protein folding and misfolding, *Nature 426*, 884−890.
6. Selkoe, D. J. (2003) Folding proteins in fatal ways, *Nature 426*, 900−904.
7. Rose, G. D., Fleming, P. J., Banavar, J. R., and Maritan, A. (2006) A backbone-based theory of protein folding, *Proc. Natl. Acad. Sci. U.S.A. 103*, 16623−16633.
8. Tucker, M. J., Oyola, R., and Gai, F. (2006) A novel fluorescent probe for protein binding and folding studies: p-Cyano-phenylalanine, *Biopolymers 83*, 571−576.
9. Tucker, M. J., Oyola, R., and Gai, F. (2005) Conformational distribution of a 14-residue peptide in solution: A fluorescence resonance energy transfer study, *J. Phys. Chem. B 109*, 4788−4795.
10. Getahun, Z., Huang, C. Y., Wang, T., De Leon, B., DeGrado, W. F., and Gai, F. (2003) Using nitrile-derivatized amino acids as infrared probes of local environment, *J. Am. Chem. Soc. 125*, 405−411.
11. Huang, C. Y., Wang, T., and Gai, F. (2003) Temperature dependence of the CN stretching vibration of a nitrile-derivatized phenylalanine in water, *Chem. Phys. Lett. 371*, 731−738.
12. Efimov, A. V. (1994) Common structural motifs in small proteins and domains, *FEBS Lett. 355*, 213−219.
13. Hoffman, D. W., Cameron, C. S., Davies, C., White, S. W., and Ramakrishnan, V. (1996) Ribosomal protein L9: A structure determination by the combined use of X-ray crystallography and NMR spectroscopy, *J. Mol. Biol. 264*, 1058−1071.
14. Kuhlman, B., Boice, J. A., Fairman, R., and Raleigh, D. P. (1998) Structure and stability of the N-terminal domain of the ribosomal protein L9: Evidence for rapid two-state folding, *Biochemistry 37*, 1025−1032.
15. Kuhlman, B., Luisi, D. L., Evans, P. A., and Raleigh, D. P. (1998) Global analysis of the effects of temperature and denaturant on the folding and unfolding kinetics of the N-terminal domain of the protein L9, *J. Mol. Biol. 284*, 1661−1670.
16. Cho, J. H., Sato, S., and Raleigh, D. P. (2004) Thermodynamics and kinetics of non-native interactions in protein folding: A single point mutant significantly stabilizes the N-terminal domain of L9 by modulating non-native interactions in the denatured state, *J. Mol. Biol. 338*, 827−837.
17. Anil, B., Sato, S., Cho, J. H., and Raleigh, D. P. (2005) Fine structure analysis of a protein folding transition state: Distinguishing between hydrophobic stabilization and specific packing, *J. Mol. Biol. 354*, 693−705.
18. Cho, J. H., and Raleigh, D. P. (2005) Mutational analysis demonstrates that specific electrostatic interactions can play a key role in the denatured state ensemble of proteins, *J. Mol. Biol. 353*, 174−185.
19. Luisi, D. L., and Raleigh, D. P. (2000) pH-dependent interactions and the stability and folding kinetics of the N-terminal domain of L9. Electrostatic interactions are only weakly formed in the transition state for folding, *J. Mol. Biol. 299*, 1091−1100.
20. Pace, C. N. (1986) Determination and analysis of urea and guanidine hydrochloride denaturation curves, *Methods Enzymol. 131*, 266−280.
21. Santoro, M. M., and Bolen, D. W. (1988) Unfolding free-energy changes determined by the linear extrapolation method. 1. Unfolding of phenylmethanesulfonyl α-chymotrypsin using different denaturants, *Biochemistry 27*, 8063−8068.
22. Vugmeyster, L., Kuhlman, B., and Raleigh, D. P. (1998) Amide proton exchange measurements as a probe of the stability and dynamics of the N-terminal domain of the ribosomal protein L9: Comparison with the intact protein, *Protein Sci. 7*, 1994−1997.
23. Myers, J. K., Pace, C. N., and Scholtz, J. M. (1995) Denaturant m values and heat capacity changes: Relation to changes in accessible surface areas of protein unfolding, *Protein Sci. 4*, 2138−2148.
24. Tanford, C. (1970) Protein denaturation. C. Theoretical models for the mechanism of denaturation, *Adv. Protein Chem. 24*, 1−95.
25. Horng, J. C., and Raleigh, D. P. (2003) ϕ-Values beyond the ribosomally encoded amino acids: Kinetic and thermodynamic consequences of incorporating trifluoromethyl amino acids in a globular protein, *J. Am. Chem. Soc. 125*, 9286−9287.
26. Anil, B., Song, B. B., Tang, Y. F., and Raleigh, D. P. (2004) Exploiting the right side of the Ramachandran plot: Substitution of glycines by D-alanine can significantly increase protein stability, *J. Am. Chem. Soc. 126*, 13194−13195.

27. Bann, J. G., and Frieden, C. (2004) Folding and domain-domain interactions of the chaperone PapD measured by F-19 NMR, *Biochemistry 43*, 13775−13786.
28. Muralidharan, V., Cho, J. H., Trester-Zedlitz, M., Kowalik, L., Chait, B. T., Raleigh, D. P., and Muir, T. W. (2004) Domain-specific incorporation of noninvasive optical probes into recombinant proteins, *J. Am. Chem. Soc. 126*, 14004−14012.
29. Schnolzer, M., Alewood, P., Jones, A., Alewood, D., and Kent, S. B. H. (1992) In situ neutralization in Boc-chemistry solid-phase peptide-synthesis: Rapid, high-yield assembly of difficult sequences, *Int. J. Pept. Protein Res. 40*, 180−193.
30. Dawson, P. E., and Kent, S. B. H. (2000) Synthesis of native proteins by chemical ligation, *Annu. Rev. Biochem. 69*, 923−960.
31. Muralidharan, V., and Muir, T. W. (2006) Protein ligation: An enabling technology for the biophysical analysis of proteins, *Nat. Methods 3*, 429−438.
32. Schultz, K. C., Supekova, L., Ryu, Y. H., Xie, J. M., Perera, R., and Schultz, P. G. (2006) A genetically encoded infrared probe, *J. Am. Chem. Soc. 128*, 13984−13985.

BI7010674